Chapter 13
Disturbance Rejection Run-to-Run Controller for Semiconductor Manufacturing

Marzieh Khakifirooz, Mahdi Fathi and Panos M. Pardalos

Abstract This chapter introduces a framework of disturbance rejection controller for discrete-time Run-to-Run (R2R) control system in semiconductor manufacturing environments. While we discussed the source of uncertainty and disturbance in wafer fabrication process, the photolithography process as one of the cutting-edge steps in wafer fabrication is selected for illustrating the power of disturbance rejection algorithm for compensating the misalignment. Along with this case study, some classification of disturbance rejection control algorithm with the structure of control plant is discussed.

13.1 Introduction

As society explores the Fourth Industrial revolution characterized by access to and leveraging of knowledge in the manufacturing enterprise, a meticulous and intelligent process control is needed to achieve higher throughput and customer satisfaction [31]. Controlling a complex system is challenging because the process components and variables operate autonomously and interoperate with other manufacturing segments. The immense in manufacturing complexity causes the several sources of measurable and unmeasurable uncertainties such as disturbance. This chapter aims to tackle the disturbances in feedback control operation in semiconductor production process by engaging the disturbance rejection models into the system.

M. Khakifirooz (✉)
Tecnológico de Monterrey, Monterrey, Mexico
e-mail: mkhakifirooz@tec.mx

M. Fathi
Mississippi State University, Starkville, MS, USA
e-mail: fathi@ise.msstate.edu

P. M. Pardalos
University of Florida, Gainesville, FL, USA
e-mail: pardalos@ise.ufl.edu

M. J. Blondin et al. (eds.), *Computational Intelligence and Optimization Methods for Control Engineering*, Springer Optimization and Its Applications 150,
https://doi.org/10.1007/978-3-030-25446-9_13

The objective of this work is to introduce readers the traditional and novel disturbance rejection systems for controlling the semiconductor manufacturing process. The paper then emphasizes on design and structure of control system with R2R architecture. It covers the technological foundations of feedback control system and addresses current threats faced by process engineers for handling the uncertainty of controlling the semiconductor production process along with existing state-of-the-art solutions for building up the disturbance-free optimization models. The topic will discuss from the perspectives of both practical implementations in the industry and cutting-edge academic research to provide a holistic mindset for process engineers and quality managers in industry, in addition to researchers and educators in the design and manufacturing communities.

The scope of this study is to build essential knowledge around control process in the semiconductor industry, the R2R control system and the disturbance rejection model, and other essentials. However, we are focusing almost exclusively on issues relevant to designing, constructing, and adapting the various disturbance rejection (free) control system for semiconductor manufacturing based on R2R control structure and optimization algorithm.

The remainder of this study is organized as follows, Section 13.2, introduces the structure of R2R feedback control system in the semiconductor industry. Section 13.3 discusses the source of uncertainties in wafer fabrication process. Section 13.4 introduces the design of disturbance rejection controllers including the structure of closed-loop system and algorithm of adaptive and robust control systems. Section 13.5, illustrates the control process of Photolithography process as one of the cutting-edge steps in wafer manufacturing and the case study of overlay error. The main challenges in Photolithography control process will discuss, and the result of reinforcement learning disturbance rejection model with traditional Exponentially Weighted Moving Average (EWMA) model will compare for further interpretation. Section 13.6, concludes the paper.

13.2 Run-to-Run Control System

The R2R control is one of the general controlling techniques in semiconductor manufacturing [38]. The primary objective of R2R control is variability reduction of the process through the shrinking the process output error. R2R control has been extensively adapted to analyze a variety of challenges in the process control of complex semiconductor manufacturing.

R2R control consists of two major steps:

1. building a linear regression model based on offline experiments between the input variable(s) u_t and the output or response variable(s) y_t.
2. estimating the process variable on online experiments, while the offline model based on the observed process and data is continuously updated and determine the control action (tuning the online model).

In semiconductor manufacturing, the number of runs for a specific product, recipe, chamber, and tool is small and collecting enough observations to fit and eventually use a model for control purposes is impossible [28]. Therefore, the control process is required the online estimation and tuning to predict the parameter setting of controller. In this case, at each machine's utilization time (in brief called run), the updated model is used to compute the control action.

Consider a single-input-single-output (SISO) control system, the basic assumption in the first step of R2R control is that the process exhibits static. This means that the output variable y_t at run t depends only on the input variable u_{t-1} at the end of run $t-1$ (when the inputs variable u_{t-1} or process output y_{t-1} at run $t-1$ has an effect on y_t the process exhibits dynamics).[1] The next assumption in the first step of R2R is that the process is modeled by fitting (optimizing) to the simple first-order linear process of the form

$$y_t = \alpha + \beta u_{t-1} + \varepsilon_t \tag{13.1}$$

where α and β are process intercept and gain (slope) parameters, ε_t is a white noise error.

After optimization within the first step, the second step tries to maintain the process variables as close as possible to the optimum (target) value. In R2R control system usually, EWMA filter is used for predicting error and feedback signal. The optimal control action for reaching the desired target T value for the process (13.1) is

$$\hat{u}_1 = \frac{T - \alpha_0}{\beta_0}. \tag{13.2}$$

where α_0 and β_0 are the initial values of α and β, respectively. Due to dynamic behavior of semiconductor industry, the basic assumption in R2R control is to having a time-varying (dynamic) intercept, α. Therefore, resulting from Eq. (13.2), the control action computes from predicted response value $\hat{y}_t = a_{t-1} + b\hat{u}_{t-1}$, where $b = \hat{\beta}$ as the gain of slope parameter estimates offline and $a_t = \hat{\alpha}_{t+1|t}$ computes recursively based on the EWMA equation

$$a_t = \lambda(y_t - b\hat{u}_{t-1}) + (1 - \lambda)a_{t-1}. \tag{13.3}$$

where λ is EWMA weighting. Figure 13.1 illustrates a block diagram of the general structure of an R2R controller. R2R controller consists of two major steps. First, at each run, a linear regression model is built to estimate the output measurement (inner loop in Fig. 13.1). The estimated model by inner loop is continuously updated and tuned based on output measurement data by the outer loop performing as a supervisor of the inner loop. In fact the outer loop takes post-process measurements and gives a control action for each run.

[1] Static model: $y_t = F(u_{t-1})$; Dynamic model: $y_t = F(y_{t-1}, u_{t-1})$.

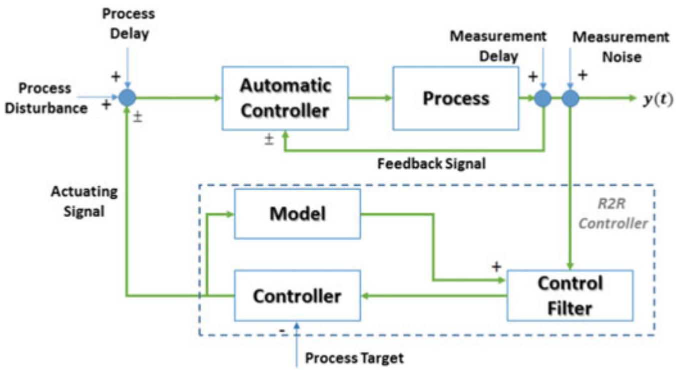

Fig. 13.1 Supervisory Run-to-Run controller

The EWMA controller is the most preferred design in R2R control. However, EWMA controller has several limitations. Some of the underlying limitations of EWMA include

- dependency on maximum likelihood estimation (MLE) of optimal decay factor,
- dependency on limited control action by fixed filtering parameters,
- dependency on multiple filtering steps,
- inefficiency to deal with the large-scale disturbance of the real-world system.

On the other hand, the traditional EWMA controller cannot satisfy the demand for high-mixed manufacturing process. Therefore, EWMA controller is not the best choice for applying in real-world case studies [29].

13.3 The Source of Disturbance in Semiconductor Industry

In wafer fabrication process, the growth or expansion of uncertainty about the health of processes and products often leads to major scrap events [28]. Thousands of products can be scrapped and generate a major production disturbance. Therefore, quality controls are required to take place at every stage of the production line, for protecting manufacturing systems from tool drift.

Industrial process models need to be identified and estimated from operating data and therefore encompass some level of uncertainty. Process variation can be caused by unmeasured disturbances (apparent in statistical models as random errors) or result from the uncertainty in model parameters, which are estimated from the data. In addition to these sources of variation, some process disturbances can be measured. However, the measured disturbances, such as process delay, are uncontrollable during actual production. Ambient temperatures and raw material variations can count as two typical examples of noise variables, which are encountered in manufacturing. Roughly speaking, uncertainty is divided into two categories:

- uncertainty in model parameters,
- uncertainty in noise variables.

Therefore, when considering a state-space system, the equation for predicting the system output, concerning the system noise and disturbance, is described as follows:

$$\begin{aligned} x_{t+1} &= C_1 x_t + C_2 u_t + d_t \\ y_{t+1} &= C_3 x_{t+1} + \varepsilon_t \end{aligned} \tag{13.4}$$

where d_t is process disturbance, x_t is states vector in state-space model for run t and C_1, C_2, and C_3 are coefficient matrices in state-space model, and y_t, u_{t-1} and ε_t are the same as (13.1).

Several studies have been implemented to reduce the effect of uncertainty on the performance of the control system. However, providing a robust solution to deal with both online variabilities of uncontrollable noise, and uncertainty in model parameters, is still an interesting and challenging research topic. Figure 13.1, merged the dynamic control system by uncertainties such as measurement noise, disturbance, process delay, and measurement delay.

13.3.1 Process Disturbance

Knowing the basics of system disturbances will assist control systems in the identification and controlling of such disturbances, which are representative of unusable parts of the actual value produced from any closed-loop system. Therefore, the efficient manner to avoid, and eliminate disturbances in the systems, is to use system feedback. The feedback loop assists to enable the control system to monitor the disturbances and processing system, to reduce, minimize, or eliminate disturbances, and achieve a state of stability in the system.

An integrated moving average ($IMA(1, 1)$) disturbance model, is widely employed in the control of discrete-part manufacturing processes [33]. Consider a process operates in closed-loop under a feedback control system. Feedback control can be employed to minimize the variability of outputs caused by invisible disturbances. In contrast, feedforward control can be used to decrease the influence of uncontrollable variables that have been measured, and which influence process variability. Sometimes, the prior knowledge as a form of Bayesian information can proceed to demonstrate the closed-loop identification.

13.3.2 Process Noise

In manufacturing processes, there are frequently, observable disturbances that can be measured during operations. Observable, but uncontrollable variables, are referred to as noise variables in process optimization literature.

Noise is an outcome of using sensor technologies or measuring process variables. Concerning electrical sensors and signals, measurement noise is often produced due to interaction with other electrical sources. Also, some physical blocking can affect sensors, resulting in incorrect signals being detected by the controller. In a typical process control situation, a proportional–integral–derivative (PID) controller can make corrective actions by reducing the proportion of the error between the process variable and the setpoint, combined with the integral and derivative, of that difference. The derivative action is most often affected by noise and disturbances.

In statistical process optimization literature, the statistical inference solutions are widely applied offline and are therefore not able to process adjustment methods, so that different controllable variable settings can be recommended, which are dependent on online noise variables and measured during production.

13.3.3 Stochastic Process Delay

The implementation of advanced process control (APC) in semiconductor manufacturing, blended with an inherent problem known as metrology delay which adversely affects R2R control performance.

Due to the need for the provision of rapid feedback to the process control, the lack of real-time metrology data causes extensive limitations in the R2R control. Most semiconductor manufacturing processes suffer from issues caused by metrology delays due to the time needed for measurements, metrology capacity, and the waiting time in the wafer queue between the processing tool and the metrology station [18]. The stability and performance of the process will be affected by the metrology delay. Moreover, since quality measurements perform online, the delay would not be fixed but flows stochastically. Several other phenomena make sever disturbance including the delay of proceeding because of bottleneck tools/processes in the system.

Thus far, numerous researches have been done in the semiconductor industry, to study on methods to reduce the effects of infrequent measurements and extensive metrology delays [16, 17, 51, 52, 55]. Virtual Metrology (VM) is deemed as the most popular technique and is a potential solution for overcoming these difficulties [34, 53].

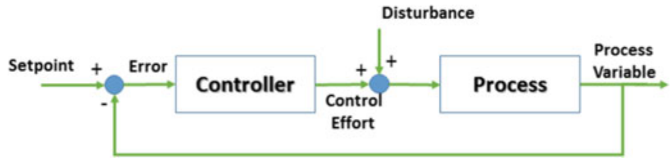

Fig. 13.2 Simple closed-loop operations diagram

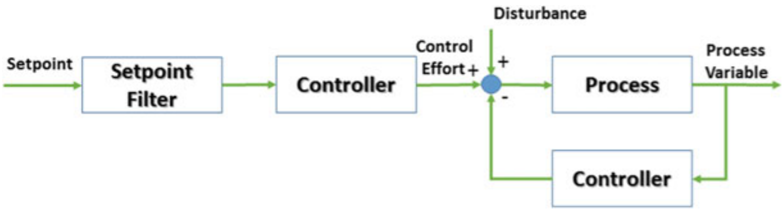

Fig. 13.3 Closed-loop operations diagram with setpoint tracker

13.4 Design of Disturbance Rejection Control System

13.4.1 Structure of Disturbance Rejection Control Systems

The closed-loop control design is the best-suited design for disturbance rejection controllers.

Consider a simple feedback controller in closed-loop mode. When a disturbance added to the system, the process variable will begin to change according to the magnitude of the load and physical characteristics of the process. However, a simple feedback controller cannot determine how the process reacts to a disturbance, because the process response to disturbance is faster than its response to setpoint change. (See the simple closed loop operations diagram in Fig. 13.2).

Regards to the dependency of the closed-loop controller to the feedback signal, this question may come to mind "what happens to the stability of system when the feedback is inadequate?" This problem can be solved when the controller can be equipped with setpoint-filtering. The setpoint-filtering allows that mathematical inertia to minimize the distance between the setpoint and output variable. (See the Closed-Loop operations diagram in Fig. 13.3).

13.4.2 Algorithms for Disturbance Rejection Control System

In control system, the algorithm mainly classifies into robust and adaptive controllers. Robust systems are expected to work well with plants which change their characteristics along time, or in noisy environments and have fixed control parameters. However,

Table 13.1 Categories of feedback adaptive and robust control

Adaptive control	Robust control
Optimal dual controllers [24]	Sliding mode control [49]
Suboptimal dual controllers [1]	Variable structure control [4, 45]
Adaptive pole placement [9]	Linear–quadratic–Gaussian control [47]
Extremum-seeking controllers [46]	Active Disturbance Rejection Control [26]
Iterative learning control [3]	Passivity based control [39]
Gain scheduling [42]	Lyapunov based control [22]
Model reference adaptive controllers [10]	Quantitative feedback theory [41]
Model identification adaptive controllers [43]	Tracking differentiator [20]
Multiple models [25, 54]	Extended state observer [21]

it is implied that those changes are somewhat bounded and the closed-loop system which encompasses the fixed robust controller presents stability, controllability, and observability.

But in scenarios where the changes in the plant are extensive, often it is not possible to design a robust controller with a fixed parameter. In this case, one uses an adaptive controller whose parameters change with time and tracks the changes in the plant, with the goal of designing a system which performs by the design constraints.

In other words, an adaptive controller has to adapt to unknown uncertainties while a robust controller has to work within a compact set known a priori of uncertainties. The goal of an adaptive controller is to estimate unknown parameters first, usually online, and then derive the control law, while the purpose of a robust controller is to formulate a control law, usually based on worst case scenario, so that the controller works for the whole range of norm-bounded disturbance, without changing the control law.

Therefore, an adaptive controller adapts to the changes in its environment and modifies the control law based on the same information, while a robust controller provides a control law that is guaranteed to work throughout the norm-bounded disturbance range, without ever changing the control law.

Adaptive and robust control comes in many variants some of them along with some references are summarized in Table 13.1.

Adaptive or robust control methods are less successful when facing dynamicity (i.e., unbounded noise, change in environmental setting) or in real time obtaining missing information (i.e., delay). In these cases, the use of artificial intelligence (AI) tools can help to expand the capacity of complex control systems by covering tasks which quantitative models enable or less efficient to solve them. A variety of artificial intelligence tools can be used individually as the control system or as an auxiliary aid for quantitative models such as: neural network control [14], Bayesian control [23], fuzzy control [56], neuro-fuzzy control [27], expert systems [15], genetic control [35], and cognitive/conscious control [12]. Figure 13.4 illustrates the implementation of levels of different control models in a complex system.

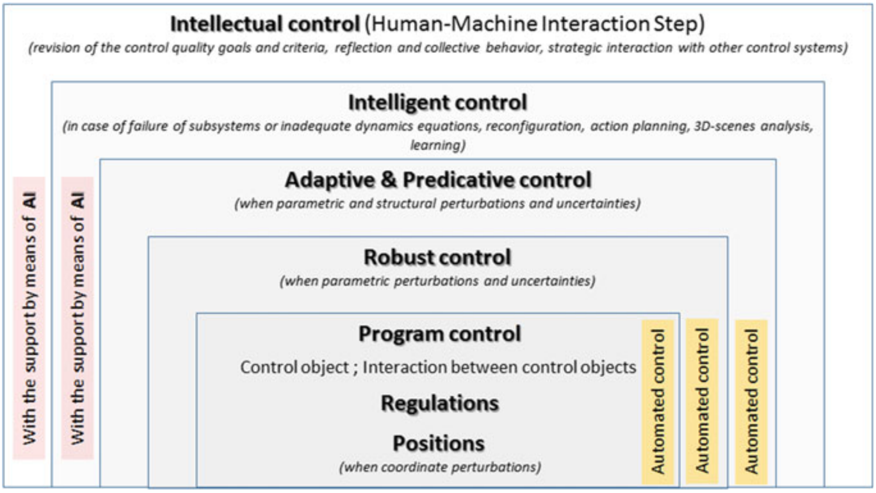

Fig. 13.4 Heterogeneous control of complex systems [50]

13.5 Case Study: Semiconductor Manufacturing and Challenges in Controlling the Patterning Process

Semiconductor device fabrication is encompassed in several processing steps. These steps are characterized by four primary sections, including patterning, etching/removal, deposition, and modification, as summarized in Table 13.2. Among these processes, the lithography process is the primary step in wafer fabrication. Following this section, some key demand features of lithography process are introduced for the analytical tools utilized in designing an adequate control system.

13.5.1 Photolithography Process

Lithography is one of the frequently used processes in fabricating chips, and typically between 30 and 35%, of the overall processing costs, and between 40 and 50%, of the completion time, is accounted for this process [37]. Additionally, the development plan for the future of lithography process required shrinkage in die size, and therefore lithography will have a technical limitation tendency when associated with the feature size reduction phenomena. Thereupon, lithography requires a high resolution, high sensitivity, precise alignment, and low defect density to achieve visions of wafer manufacturing. Therefore, setting up an accurate control system with high impact on disturbance rejection is an essential appliance for the lithography process.

Currently, the step-and-scan (shortened scanner) method is one of the most commercially used systems, in the lithography process. The purpose of the scanner is

Table 13.2 Semiconductor device fabrication steps

Process	Methods
Deposition: Grows, coats, or transfers a material onto the wafer	Physical vapor deposition
	Chemical vapor deposition
	Electrochemical deposition
	Molecular beam deposition
	Atomic layer deposition
Removal: Removes material from the wafer either in bulk mode or selectively	Wet etching
	Dry etching
	Chemical–mechanical planarization
Patterning: Shapes or alters the shape of the deposited materials	Lithography
Modification: Doped transistor sources and drains	Ion implantation
	Rapid thermal anneals
	Ultraviolet light processing

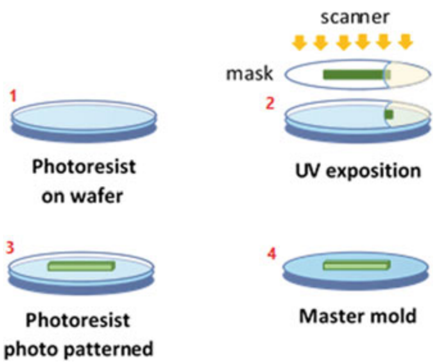

Fig. 13.5 Wafer fabrication in photolithography process

to superimpose a masking pattern on top of the existing wafer pattern. Figure 13.5 illustrates the initial steps of wafer fabrication in the photolithography process when using the scanner. The gap between the actual position of the mask over the actual position of the wafer substrate is known as the overlay error [5, 6]. As is evident from research, the overlay error has proven to be the most challenging issue in the photolithography process [2, 6, 40, 44].

13.5.1.1 Overlay Error

As discussed earlier, during semiconductor fabrication process, each wafer goes several times under the photolithography process, and at each time a layer of photo-

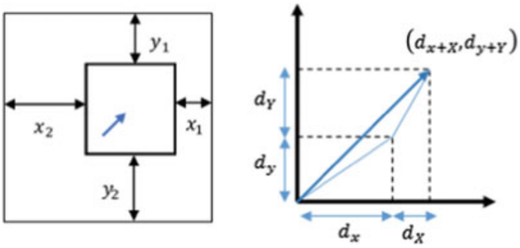

Fig. 13.6 The overlay error measurement [8]

resist material exposure on the surface of wafer. The misalignment between the current and previous exposure layers, through the box-in-box design is called overlay error. When the inside box is accurately patterned in the center of the outside box, no overlay errors are apparent (Fig. 13.6).

The response variables of the overlay error, are indicated as follows:

$$\begin{aligned} d(x+X) &= \tfrac{x_1 - x_2}{2} \\ d(y+Y) &= \tfrac{y_1 - y_2}{2} \end{aligned} \tag{13.5}$$

where (x, y) is intrafield coordinate system, regarding the center of the field[2] and (X, Y) is interfield coordinate system, regarding the center of the wafer. In Fig. 13.6, dx and dy denote to interfield overlay error in x and y direction, respectively, and dX and dY denote to interfield overlay error in X and Y direction, respectively.

The presence of overlay errors can be attributed to intrafield and interfield errors [7]. The interfield overlay errors are the result of the mismatch between the patterning mask and wafer. The intrafield errors are due to fitment problems between the lens of the scanner (light source), and the patterning mask. The interfield errors are measured at the center of the wafer, and the intrafield errors at the center of the exposure. The variables leading to intrafield, and interfield overlay errors, are presented in Fig. 13.7 and Fig. 13.8, respectively.

Various feedback controllers are designed based on R2R control for compensating the misalignment during the photolithography process. The most commonly applied and theoretical method is formed on EWMA estimation, other learning-based models are Kalman filters [11], artificial neural networks [32], machine learning [30], and PID controller [8]. Following this study, we introduce a new approach for compensating overlay error which has an advantage for faster disturbance rejection in comparison to the EWMA, PID, or Kalman filters based on reinforcement learning optimization.

---

[2] The surface of a wafer can be partitioned into smaller part for increase the accuracy of measurement the overlay error, each partition is called a field.

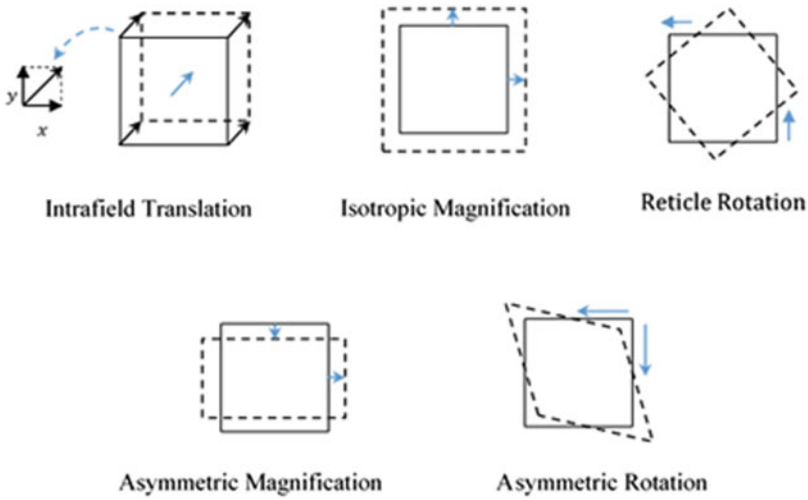

Fig. 13.7 Variables leading to intrafield overlay error [7]

Fig. 13.8 Variables leading to interfield overlay error [7]

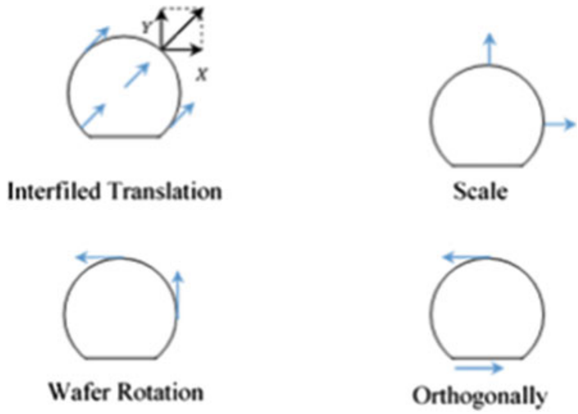

13.5.2 Reinforcement Learning Optimization

A partially observable Markov decision process (POMDP) [36] is a generalization of Markov decision process (MDP) [48] which only part of the information is available about the current state, and this led to the uncertainties (i.e., delay, noise).

Consider a class of algorithms for finding good approximations to a class of learning problems in which agents interact in a dynamic, noisy and stochastic environment; this interaction is conventionally modeled as an POMDP which consists of

- S_t: a finite set of states.
- A_t: a finite set of actions.
- $R(S_t, A_t)$: a reward function.

- $P(S_{t+1}|S_t, A_t)$: a state transition probability function.
- O_t: a set of observations.
- $P(O_{t+1}|S_{t+1}, A_t)$: an observation probability.
- $r_t \in [0, 1]$: a discount factor.
- B_t: a distribution over state S_t called "Belief State".

POMDP can identify as an optimal or near-optimal behavior for an uncertain system. The MDP problem seeks to find a mapping from states to actions; however, the challenge in POMDP problem is to find a mapping from probability distributions over states to actions. For achieving this purpose, the key step is to calculate the value function of a given policy (π) which is the mapping function from the state to the action, to maximize the expected sum of the discounted factor. Regards to the definition of POMDP components described in above the optimization procedure of POMDP is following below steps:

1. set up the unobserved state S_t of the system at each time step t
2. select an action A_t,
3. maintain the distribution over S_t as B_t,
4. receive the reward function $R(S_t, A_t)$,
5. transitions to unobserved state S_{t+1} with probability $P(S_{t+1}|S_t, A_t)$,
6. receive an observation O_{t+1} with probability $P(O_{t+1}|S_{t+1}, A_t)$,
7. estimate a distribution on state S_{t+1} as $B_{t+1}(S_{t+1}) = P(S_{t+1}|O_{t+1}, A_t, B_t(S_t))$,
8. update the reward function by $R(S_{t+1}, A_{t+1}) = B_{t+1}(S_{t+1}) \times R(S_t, A_t)$
9. optimize the return function by policy $\pi(S_{t+1}) = \max_{A_{t+1}} \sum r_{t+1} R(S_{t+1}, A_{t+1})$ and select the best action A_{t+1},
10. update and repeat the process.

The Bellman's optimality [19] equation says that under principal of stochastic approximation, the average bias $Q(S_t, A_t)$ (Q-learning) from t times simulation-based solution is

$$Q(S_t, A_t) = \min_{A_t} \left[R(S_t, A_t) - \frac{1}{t} E\left\{ \sum_t R(S_t, A_t) \right\} + \sum_t P(S_t|S_{t-1}, A_{t-1}) \right.$$
$$\left. \times E\left\{ \sum_t R(S_t, A_t) - \frac{1}{t} E\left\{ \sum_t R(S_t, A_t) \right\} \right\} \right] \tag{13.6}$$

The POMDP relies on defining the set of states and their expected values, the action transition matrix and reward structure. The description, role, and action of each component in details for the control system of overlay model are summarized as follows[3]:

The state-space: The output of the controller to the plant ($\mathbf{x}_t$), given the action ($\mathbf{u}_t$), including the disturbance and process delay. Considering N overlay factors, therefore, there are $1 \times N$ different states in the system. Note that in practice the actual value of $\mathbf{x}_t$ is predictable, and not observable.

The observation space: The actual output of the plant ($\mathbf{y}_t$) for N overlay factors including the metrology delay and measurement noise.

The action transition matrix: The matrix of probability which each sate ($\mathbf{x}_t$) can appear in the sequence of the lithography process. Respecting the definition of variables in (13.4) the elements of transition matrix can be derived by

$$P(\mathbf{x}_t|\mathbf{x}_{t-1}, \mathbf{u}_{t-1}). \tag{13.7}$$

The transition matrix can be computed based on the historical data and update after each run.

Belief updating: The probability distribution over $\mathbf{x}_t$ given the state of previous belief and observation and action at the current run.

$$B(\mathbf{x}_t) = \frac{P(\mathbf{y}_{t-1}|\mathbf{x}_{t-1},\mathbf{u}_{t-1}) \sum_t P(\mathbf{x}_t|\mathbf{x}_{t-1},\mathbf{u}_{t-1})B(\mathbf{x}_{t-1})}{\sum_t P(\mathbf{y}_{t-1}|\mathbf{x}_{t-1},\mathbf{u}_{t-1})P(\mathbf{x}_t|\mathbf{x}_{t-1},\mathbf{u}_{t-1})B(\mathbf{x}_{t-1})}. \tag{13.8}$$

Reward function: The actual error which results from action $\mathbf{u}_t$ is

$$\mathbf{E}_t = \mathbf{y}_t - T \tag{13.9}$$

Average bias: The optimal value of actual error after t run with regards to the transition matrix at each run and learning from the previous runs. Since each action is independent, the only factor that influences the total error is the gain of the actions. Therefore, bias is interpreted as the expected total difference between the reward ($\mathbf{E}_t$) and the gain ($G(\mathbf{E}_t)$).

$$bias = \mathrm{E}\left\{\sum_t \mathbf{E}_t - G(\mathbf{E}_t)\right\} \tag{13.10}$$

In practice when $t \to \infty$, the optimal gain is $\frac{1}{t}\mathrm{E}\left\{\sum_t \mathbf{E}_t\right\}$.

Consider $\mathbf{y}_t$, where $T = 0$ in (13.9) as reward function in tth run then the average optimality reward function based on [13] is

$$Q(\mathbf{x}_t, \mathbf{u}_t) = (1 - \eta_t)Q(\mathbf{x}_{t-1}, \mathbf{u}_{t-1}) + \eta_t \times \left[\mathbf{y}_t - G(\mathbf{y}_t) + \min_{\mathbf{u}_t} Q(\mathbf{x}_{t-1}, \mathbf{u}_{t-1})\right], \tag{13.11}$$

[3]Regards to notation in the beginning of this section $\mathbf{x}_t$ is equivalent to S_t; $\mathbf{u}_t$ is A_t; $\mathbf{y}_t$ is O_t; $P(\mathbf{x}_t|\mathbf{x}_{t-1}, \mathbf{u}_{t-1})$ is $R(S_t|S_{t-1}, A_{t-1})$; and E_t is $R(S_t, A_t)$.

where $G(\mathbf{y}_t)$ can be learned and updated at each run by

$$G(\mathbf{y}_t) = (1 - \eta'_t)G(\mathbf{y}_{t-1}) + \eta'_t \left[\frac{(t-1)G(\mathbf{y}_{t-1}) + \mathbf{y}_t}{t} \right] \tag{13.12}$$

The learning parameters η_t and η'_t (similar to λ in EWMA controller) are both decayed at run t by the following rule:

$$\eta_t, \eta'_t = \frac{\eta_0, \eta'_0}{1 + \frac{t^2}{K+t}} \tag{13.13}$$

where K is a very large number, and η_0, η'_0 are initial values for learning parameter η and η', respectively.

Choosing the optimal action: The objective function of a control system in (13.9) can be minimize by the optimal solution of stationary policy given by the observation space:

$$\pi(B(\mathbf{x}_t)) = \arg\min_{r_t} \left[r_t B(\mathbf{x}_t) \times Q(\mathbf{x}_t, \mathbf{u}_t) r'_t \right]. \tag{13.14}$$

Using the model as a controller: For having a controllable and observable system, the following assumptions should be satisfied:

- The model applies over an infinite number of runs, implying that the control system is stationary.
- Conditioned on the true $\mathbf{u}_t$ and control setting at run t, the $P(\mathbf{y}_t|\mathbf{x}_t)$ is independent from information related to the run $t-1$.
- The measurement noise and process disturbance are accumulated to the $\mathbf{y}_t$ and $\mathbf{u}_t$, respectively.
- Regards to policy function in (13.8), objective function of optimization goal in (13.9) is updated by

$$\arg\min_{r_t} \sum_t \{ r_t B(\mathbf{x}_t) \times Q(\mathbf{x}_t, \mathbf{u}_t) r_t \} \tag{13.15}$$

For investigating the efficiency of the POMDP controller in comparison with EWMA as the most common control filter in the semiconductor industry, an SISO process with 200 runs simulated as follows:

- generating 200 runs of uncontrollable disturbance d_t and noise ε_t from $N(0, 1)$ based on the model in (13.4), where y_1, u_1, x_1 and T are set to zero.
- fitting simulated overlay errors from 200 runs into (13.4) and obtaining the effect of cumulative disturbance on y_t, u_t, and x_t for run $t = 2, \ldots, 200$ where the coefficient parameters (C_1, C_2, C_3) for simplicity set to one.

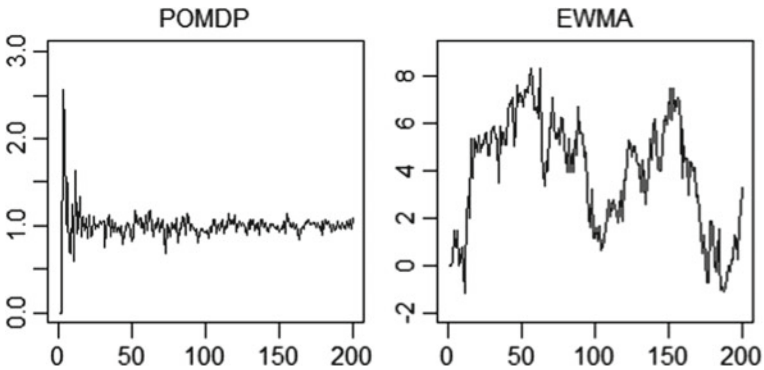

Fig. 13.9 The power of disturbance rejection between POMDP and EWMA controller. Y axis denotes to the total overlay error and X axis to the simulation runs

- calculate the probability distribution function in (13.7) based on empirical distribution function (in reality, we can use historical data to find the distribution function of $\mathbf{x}_t$).
- optimize objective function in (13.14) subject to model in (13.4) for each run where both η_0, η_0' are set to 0.5, and $K = 10^{15}$.
- evaluating the performance of the proposed POMDP controller with 200 runs in comparison with EWMA controller with fixed discount factor equal to 0.3 and $b = 0.5$ as presented in Eqs. (13.1)–(13.3) with $\varepsilon_t = 0$ (note that the effect of noise and disturbance is considered in steps 1 and 2).

Figure 13.9 illustrates this comparison based on the value of (13.9) and shows that how POMDP is performing supremely better than EWMA to compensate the disturbance.

13.6 Conclusion

This study highlighted the importance of disturbance rejection algorithm in semiconductor manufacturing for overlay error minimization during the photolithography process. The research summarized several disturbance rejection algorithms as a comprehensive collection for researchers and practitioners who would like to investigate in this field. However, the algorithm and methods for disturbance rejection are not limited to those are mentioned in this paper. Practically, the hybrid algorithm and technology-enabled method is more efficient than traditional control theory and are more applicable in the smart manufacturing environment.

References

1. Åström, K.J., Wittenmark, B.: Adaptive Control. Courier Corporation (2013)
2. Bode, C., Ko, B., Edgar, T.: Run-to-run control and performance monitoring of overlay in semiconductor manufacturing. Control Eng. Pract. **12**(7), 893–900 (2004)
3. Chen, Y., Moore, K.L., Ahn, H.S.: Iterative learning control. In: Encyclopedia of the Sciences of Learning. Springer, pp. 1648–1652 (2012)
4. Chiang, Y.C., Cheng, C.C.: Terminal adaptive output feedback variable structure control. In: IET Control Theory & Applications (2018)
5. Chien, C.F., Hsu, C.Y.: Unison analysis to model and reduce step-and-scan overlay errors for semiconductor manufacturing. J. Intell. Manuf. **22**(3), 399–412 (2011)
6. Chien, C.F., Chang, K.H., Chen, C.P.: Design of a sampling strategy for measuring and compensating for overlay errors in semiconductor manufacturing. Int. J. Prod. Res. **41**(11), 2547–2561 (2003)
7. Chien, C.F., Chang, K.H., Chen, C.P., Lin, S.L.: Overlay error model, sampling strategy and associated equipment for implementation. US Patent 6,975,974 (2005)
8. Chien, C.F., Chen, Y.J., Hsu, C.Y., Wang, H.K.: Overlay error compensation using advanced process control with dynamically adjusted proportional-integral R2R controller. IEEE Tran. Autom. Sci. Eng. **11**(2), 473–484 (2014)
9. Da Silva, F.D.C., De Oliveira, J.B., De Araujo, A.D.: Robust interval adaptive pole-placement controller based on variable structure systems theory. In: 2017 25th International Conference on Systems Engineering (ICSEng). IEEE, pp. 45–54 (2017)
10. Duarte-Mermoud, M.A., Aguila-Camacho, N., Gallegos, J.A., Travieso-Torres, J.C.: Fractional-order model reference adaptive controllers for first-order integer plants. In: New Perspectives and Applications of Modern Control Theory. Springer, pp. 121–151 (2018)
11. El Chemali, C., Freudenberg, J., Hankinson, M., Collison, W., Ni, T.: Critical dimension control of a plasma etch process by integrating feedforward and feedback run-to-run control. J. Vac. Sci. Technol. B: Microelectron. Nanometer Struct. Process. Meas. Phenom. **21**(6), 2304–2312 (2003)
12. Gamez, D.: Progress in machine consciousness. Conscious. Cogn. **17**(3), 887–910 (2008)
13. Ganesan, R., Das, T.K., Ramachandran, K.M.: A multiresolution analysis-assisted reinforcement learning approach to run-by-run control. IEEE Trans. Autom. Sci. Eng. **4**(2), 182–193 (2007)
14. Ge, S.S., Hang, C.C., Lee, T.H., Zhang, T.: Stable Adaptive Neural Network Control, vol 13. Springer Science & Business Media (2013)
15. Giarratano, J.C., Riley, G.: Expert Systems: Principles and Programming. Brooks/Cole Publishing Co. (1989)
16. Gong, Q., Yang, G., Pan, C., Chen, Y.: Performance analysis of single ewma controller subject to metrology delay under dynamic models. IISE Trans. **50**(2), 88–98 (2018)
17. Gong, Q.S., Yang, G.K., Pan, C.C., Lee, M.S.: Stability and control performance analysis of double ewma controller with metrology delay. IEEE Trans. Semicond. Manuf. **29**(1), 9–16 (2016)
18. Good, R.P., Qin, S.J.: On the stability of MIMO EWMA run-to-run controllers with metrology delay. IEEE Trans. Semicond. Manuf. **19**(1), 78–86 (2006)
19. Gross, E.: On the Bellman's principle of optimality. Phys. A: Stat. Mech. Appl. **462**, 217–221 (2016)
20. Guo, B.Z., Zhao, Z.L.: On convergence of tracking differentiator. Int. J. Control **84**(4), 693–701 (2011)
21. Guo, B.Z., Zhao, Z.L.: Extended state observer. In: Active Disturbance Rejection Control for Nonlinear Systems: An Introduction, pp. 93–154 (2016)
22. Haddad, W.M., Chellaboina, V.: Nonlinear Dynamical Systems and Control: A Lyapunov-Based Approach. Princeton University Press (2011)
23. van Hee, K.M., Hee, K.: Bayesian Control of Markov Chains, vol. 95. Mathematisch centrum Amsterdam, The Netherlands (1978)

24. Heirung, T.A.N., Ydstie, B.E., Foss, B.: Dual adaptive model predictive control. Automatica **80**, 340–348 (2017)
25. Huang, M., Wang, X., Lu, Z., Ma, L., Su, H., Wang, L.: Multiple model adaptive control for a class of nonlinear systems with unknown control directions. Int. J. Control 1–13 (2018)
26. Huang, Y., Xue, W.: Active disturbance rejection control: methodology and theoretical analysis. ISA Trans. **53**(4), 963–976 (2014)
27. Jang, J.S., Sun, C.T.: Neuro-fuzzy modeling and control. Proc. IEEE **83**(3), 378–406 (1995)
28. Khakifirooz, M., Chien, C.F., Chen, Y.J.: Bayesian inference for mining semiconductor manufacturing big data for yield enhancement and smart production to empower industry 4.0. Appl. Soft Comput. **68**, 990–999 (2018)
29. Khakifirooz, M., Fathi, M., Chien, C.F.: Modelling and decision support system for intelligent manufacturing: an empirical study for feedforward-feedback learning-based run-to-run controller for semiconductor dry-etching process. Int. J. Ind. Eng. Theory Appl. Pract. **25**(6) (2018)
30. Khakifirooz, M., Chien, C.F., Fathi, M.: Compensating misalignment using dynamic random-effect control system: a case of high-mixed wafer fabrication. IEEE Trans. Autom. Sci. Eng. (2019)
31. Khakifirooz, M., Cayard, D., Chien, C.F., Fathi, M.: A system dynamic model for implementation of industry 4.0. In: 2018 International Conference on System Science and Engineering (ICSSE). IEEE, pp. 1–6, June 2018
32. Kuo, H.F., Faricha, A.: Artificial neural network for diffraction based overlay measurement. IEEE Access **4**, 7479–7486 (2016)
33. Liptk, B.: Process Control: Instrument Engineers Handbook (2013)
34. Lynn, S.A., MacGearailt, N., Ringwood, J.V.: Real-time virtual metrology and control for plasma etch. J. Process Control **22**(4), 666–676 (2012)
35. Mitchell, M.: An Introduction to Genetic Algorithms. MIT Press (1998)
36. Monahan, G.E.: State of the art-a survey of partially observable Markov decision processes: theory, models, and algorithms. Manag. Sci. **28**(1), 1–16 (1982)
37. Moreau, W.M.: Semiconductor Lithography: Principles, Practices, and Materials. Springer Science & Business Media (2012)
38. Moyne, J., Del Castillo, E., Hurwitz, A.M.: Run-to-Run Control in Semiconductor Manufacturing. CRC Press (2000)
39. Ortega, R., Perez, J.A.L., Nicklasson, P.J., Sira-Ramirez, H.J.: Passivity-Based Control of Euler-Lagrange Systems: Mechanical, Electrical and Electromechanical Applications. Springer Science & Business Media (2013)
40. Park, S.J., Lee, M.S., Shin, S.Y., Cho, K.H., Lim, J.T., Cho, B.S., Jei, Y.H., Kim, M.K., Park, C.H.: Run-to-run overlay control of steppers in semiconductor manufacturing systems based on history data analysis and neural network modeling. IEEE Trans. Semicond. Manuf. **18**(4), 605–613 (2005)
41. Rico-Azagra, J., Gil-Martínez, M., Rico, R., Maisterra, P.: Qft bounds for robust stability specifications defined on the open-loop function. Int. J. Robust Nonlinear Control **28**(3), 1116–1125 (2018)
42. Rugh, W.J., Shamma, J.S.: Research on gain scheduling. Automatica **36**(10), 1401–1425 (2000)
43. Schreier, M.: Modeling and adaptive control of a quadrotor. In: 2012 International Conference on Mechatronics and Automation (ICMA). IEEE, pp. 383–390 (2012)
44. Sullivan, N.T.: Semiconductor pattern overlay. In: Handbook of Critical Dimension Metrology and Process Control: A Critical Review. International Society for Optics and Photonics, vol. 10274, p. 102740C (1994)
45. Sun, L., Lu, J., Liu, Y., Huang, T., Alsaadi, F.E., Hayat, T.: Variable structure controller design for Boolean networks. Neural Netw. **97**, 107–115 (2018)
46. Tan, Y., Moase, W., Manzie, C., Nešić, D., Mareels, I.: Extremum seeking from 1922 to 2010. In: 2010 29th Chinese Control Conference (CCC). IEEE, pp. 14–26 (2010)
47. Tanaka, T., Esfahani, P.M., Mitter, S.K.: LQG control with minimum directed information: semidefinite programming approach. IEEE Trans. Autom. Control **63**(1), 37–52 (2018)

48. Thie, P.R.: Markov Decision Processes. Comap, Incorporated (1983)
49. Utkin, V., Guldner, J., Shi, J.: Sliding Mode Control in Electro-Mechanical Systems. CRC Press (2009)
50. Vassilyev, S., Kelina, A.Y., Kudinov, Y., Pashchenko, F.: Intelligent control systems. Procedia Comput. Sci. **103**, 623–628 (2017)
51. Wan, L., Tan, F., Th, P.A.N.: Online estimation of time-varying metrology delay and run-to-run control co-design. Control Theory Appl. **1**, 012 (2016)
52. Wang, Y., Zheng, Y., Fang, H., Wang, Y.: Armax model based run-to-run fault diagnosis approach for batch manufacturing process with metrology delay. Int. J. Prod. Res. **52**(10), 2915–2930 (2014)
53. Wu, W.M., Cheng, F.T., Lin, T.H., Zeng, D.L., Chen, J.F.: Selection schemes of dual virtual-metrology outputs for enhancing prediction accuracy. IEEE Trans. Autom. Sci. Eng. **8**(2), 311–318 (2011)
54. Xie, J., Yang, D., Zhao, J.: Multiple model adaptive control for switched linear systems: a two-layer switching strategy. Int. J. Robust Nonlinear Control **28**(6), 2276–2297 (2018)
55. Zheng, Y., Wong, D.S.H., Wang, Y.W., Fang, H.: Takagi-Sugeno model based analysis of EWMA RtR control of batch processes with stochastic metrology delay and mixed products. IEEE Trans. Cybern. **44**(7), 1155–1168 (2014)
56. Zimmermann, H.J.: Fuzzy control. In: Fuzzy Set Theory-and Its Applications. Springer, pp. 203–240 (1996)